International Journal of Thermal Sciences 49 (2010) 611–620

Contents lists available at ScienceDirect

International Journal of Thermal Sciences

journal homepage: www.elsevier.com/locate/ijts

Study on a silica gel–water adsorption chiller integrated with a closed wet cooling tower

C.J. Chen, R.Z. Wang*, Z.Z. Xia, J.K. Kiplagat

Institute of Refrigeration and Cryogenics, Shanghai Jiao Tong University, 800 Dongchuan Road, Shanghai 200240, China

ARTICLE INFO

Article history:
Received 26 March 2009
Received in revised form
28 September 2009
Accepted 28 September 2009
Available online 28 October 2009

Keywords:
Silica gel
Water
Adsorption
Refrigeration
Cooling tower

ABSTRACT

A silica gel–water adsorption chiller integrated with a closed wet cooling tower is proposed. This adsorption chiller consists of two vacuum chambers, each with one adsorber, one condenser and one evaporator. Vacuum valves were not adopted in this chiller in order to enhance the reliability. A novel heat recovery process was carried out after a mass recovery-like process to improve the coefficient of performance (COP). Integration of the closed wet cooling tower into the chiller could ensure the cleanliness of cooling water circulating in the chiller and also promote the convenient setup of the chiller. A transient one-dimensional mathematical model was adopted to study this adsorption chiller. The simulated results showed that the cooling power and COP were 10.76 kW and 0.51 respectively when the hot water inlet temperature, the chilled water inlet temperature, the air inlet wet bulb temperature and dry bulb temperature were 85, 15, 28 and 30 °C respectively.

1. Introduction

Adsorption refrigeration systems have attracted more and more attention in research and development. These systems have two main advantages, compared to traditional vapor compression systems. Firstly, adsorption refrigeration systems employ natural substances as refrigerant, such as water, methanol and ammonia among others, which have zero GWP and ODP. Secondly, adsorption refrigeration systems can be powered with waste heat or solar energy, hence could contribute greatly to electricity energy conservation. However, adsorption refrigeration systems show a lower COP compared to absorption refrigeration systems.

One of the most prospective adsorption refrigeration systems is silica gel–water adsorption refrigeration systems. According to the References [1–3], the lumped-parameter model used to study a silica gel–water adsorption chiller could not explain the outlet temperature profiles of the working fluids during the heat recovery process, which resulted in an overestimate of COP and an underestimate of cooling power at long cycle times. As a result, a transient distributed-parameter model was employed to study the chiller [3]. The Energy balance models for the adsorber in the distributed-parameter model were divided into four parts: adsorbent, fin, metal tube and heat transfer fluids. Compared to lumped-parameter model, the transient distributed-parameter model showed a better agreement with the experimental data during the heat recovery process. A dynamic model was also employed by Saha et al. to study $CaCl_2$-in-silca gel–water adsorption chiller [4]. The Tóth's equation was used as the adsorption equilibrium equation for both silica gel–water and SWS-lL-water adsorption chiller. Di et al. [5] adopted a lumped-parameter model to study a silica gel–water adsorption chiller under variable heat source temperatures. In his model, the adsorption/desorption process was taken as an isobaric process. The calculated results for the outlet temperature of the heat transfer fluids showed a large deviation with the experimental data during the heat and mass recovery process.

Cooling towers are widely adopted in refrigeration and air-conditioning systems to reject heat to the atmosphere. Typically in solar powered absorption/adsorption cooling systems, small scale cooling towers integrated with the cooling systems are of great necessary in order to reduce the electricity consumption and promote the installation's convenience [6]. Cooling towers can be basically classified into two types: open cooling towers and closed cooling towers. In a closed wet cooling tower, cooling water flows inside the heat transfer tubes and is cooled by the spray water and airflow outside the tubes. Different from an open cooling tower, cooling water does not contact the ambient air in a closed cooling tower. As a result, the cleanliness of the cooling water can be ensured. Most of mathematical models for cooling towers are based on Merkel's theory assuming a Lewis number equal to one and neglecting the mass losses of spray water due to the evaporation of

* Corresponding author. Tel./fax: +86 21 34206548.
E-mail address: rzwang@sjtu.edu.cn (R.Z. Wang).

1290-0729/$ – see front matter © 2009 Elsevier Masson SAS. All rights reserved.
doi:10.1016/j.ijthermalsci.2009.09.009

Nomenclature

A	heat transfer area (m^2)
$\overline{A}$	mass transfer area (m^2)
$A(T_a)$	coefficient of adsorption equilibrium equation
$B(T_a)$	coefficient of adsorption equilibrium equation
C_p	specific heat capacity (J kg^{-1} K^{-1})
COP	coefficient of performance
D_{so}	pre-exponent constant (m^2 s^{-1})
E_a	activation energy of surface diffusion (J mol^{-1})
G	mass flow rate (kg s^{-1})
h	heat transfer coefficient (W m^{-2} K^{-1})
$\overline{h}$	mass transfer coefficient (kg m^{-2} s^{-1})
l	length (m)
L	latent heat of vaporization (J kg^{-1})
Le	Lewis number
M	mass (kg)
P	pressure (Pa)
Q_h	heating power (kW)
Q_r	cooling capacity (kW)
R	gas constant (J mol^{-1} K^{-1})
R_p	average radius of silica gel (m)
T	temperature (°C)
w	humidity ratio (kg H_2O kg^{-1}) dry air
X^*	equilibrium water uptake of silica gel (kg H_2O kg^{-1} dry adsorbent)
X	water uptake of silica gel (kg H_2O kg^{-1} dry adsorbent)

Greek symbols

τ	time (s)
ΔH	adsorption/desorption heat (J kg^{-1})
φ	relative humidity

Subscript

a	adsorbent
ad	adsorber
air	airflow
c	condenser
chilled	chilled water
cham	chamber
db	dry bulb
e	evaporator/evaporating
f	fluid
hot	hot water
hmtu	heat and mass transfer unit
htu	heat transfer unit
i	initial
in	inlet
m	metal
out	outlet
sw	spray water
w	water
wb	wet bulb
wv	water vapor
x	*x* direction

spray water into airflow. On the basis of Merkel theory, a simplified model was presented by Stabat and Marchio for a closed wet cooling tower [7]. In this model, water film temperature was assumed to be constant along the whole coil. However, this model did not show the outlet humidity-ratio. Thus the outlet air was considered to be saturated while calculating the evaporation rate of the spray water. Based on the enthalpy analysis of the working fluids of closed wet cooling towers, Hasan and Sirén adopted a steady-state mathematical model to optimize coefficient of performance of these cooling towers [8]. This model assumed that the inlet spray water temperature was equal to the outlet spray water temperature, which resulted in none spray water heat transfer during the calculation. Wu et al. employed a one-dimensional mathematical model to study the heat and mass transfer in a direct evaporative cooler [9]. The model was proposed based on the assumption that the sensible heat removed from air was equal to the latent heat gained from spray water evaporation. According to the model, the changes of temperature and humidity ratio of moisture air along the flowing direction of the air can be obtained.

Based on the adsorption chillers developed in Shanghai Jiao Tong University [10,11], a silica gel–water adsorption chiller integrated with a closed wet cooling tower was designed. The aim of this paper is to propose the compact adsorption chiller and to carry out a dynamic modeling of the adsorption chiller together with the cooling tower.

2. System description

The schematic diagram of the silica gel–water adsorption chiller integrated with a closed wet cooling tower is shown in Fig. 1. This compact adsorption chiller is composed of two vacuum chambers, one chilled water tank and one cooling tower. Each vacuum chamber contains one adsorber, one condenser and one evaporator. Five three-way valves (V1 ~ V5) and three solenoid valves (V6 ~ V8) are adopted in this chiller. All the valves used are water valves while vacuum valves are not adopted to enhance the reliability.

The studied cooling tower is composed of two main parts: the heat and mass transfer unit (HMTU) and the heat transfer unit (HTU). In the HMTU, 280 horizontal copper tubes are fixed in 14 vertical rows with a rectangular-pitch arrangement. The copper tubes of 9.52 mm external diameter are 1.0 m in length. Below each vertical row of copper tubes, three rows of plastic tubes with the same size as the copper tubes are arranged. The horizontal and vertical tube pitches are 20.0 and 12.52 mm respectively. Cooling water flows inside the copper tubes rather than the plastic tubes, and is cooled by spray water. The spray water is chilled due to the heat and mass transfer with the airflow on the outside surface of both the copper tubes and the plastic tubes. The air flows through the horizontal tube bundles at an opposite directions with the spray water. Thus the mass transfer area between the spray water and the airflow is about 3 times larger than the heat transfer area between the cooling water and the spray water. In the HTU, there are also 280 horizontal copper tubes arranged in 14 vertical rows while plastic tubes are not adopted. The cooling water flows through the copper tubes and is cooled by the spray water coming from the HMTU.

3. Working principle

The cycle process of this compact adsorption chiller consists of adsorption/desorption processes, mass recovery-like processes and heat recovery processes. The schematic drawing of the working processes of the studied adsorption chiller is shown in Fig. 2. Take the first process for example, hot water flows through *adsorber 2* via V4 and then goes back to a hot water tank through V3. At the same time, cooling water coming from the cooling tower flows into *condenser 2* through V1 and then rushes into *adsorber 1*, finally runs back to the cooling tower via V2. Simultaneously, chilled water goes through *evaporator 1* via V5 and then flows back to the

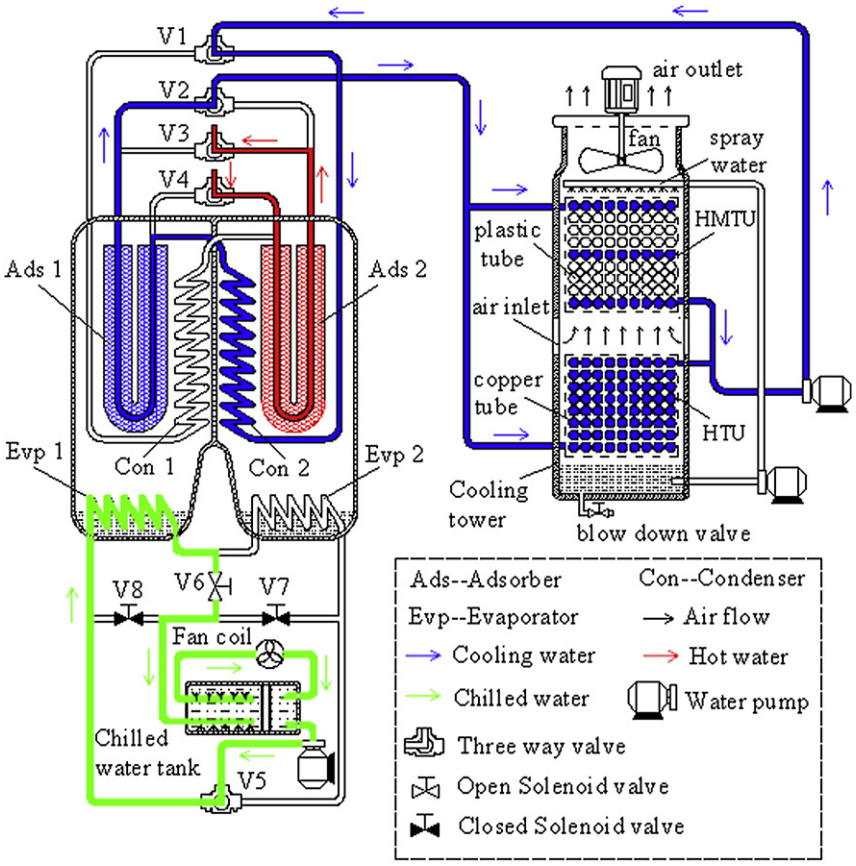

Fig. 1. Schematic diagram of the compact silica gel–water chiller integrated with a closed wet cooling tower.

chilled water tank through V6. The six processes can be described consecutively as follows:

1) Adsorber 1 works in adsorption process and adsorber 2 is in desorption process

Hot water flows into *adsorber 2* via V4 and then goes back to the hot water tank through V3. The desorbed water vapor from the *adsorber 2* firstly condenses in *evaporator 2* since temperature of the *evaporator 2* is lower than that of *condenser 2*. When pressure of desorption chamber (the right vacuum chamber) is higher than the saturation pressure under the temperature of the *condenser 2*, condensation will occur in the *condenser 2*. Finally, the condensate flows downwards into the *evaporator 2*. Simultaneously, *adsorber 1* is cooled by cooling water from the *condenser 2* and adsorbs water (refrigerant) from *evaporator 1*. Chilled water passes through the *evaporator 1* via V5 and is cooled due to the evaporation of the refrigerant in the *evaporator 1*. Finally the chilled water flows back to the chilled water tank through V6.

2) Mass recovery-like process (Heat recovery from evaporator 2 to evaporator 1)

After the first process, a heat recovery process from the *evaporator 2* to the *evaporator 1* starts via the switch of V5, V6 and V8. Chilled water from the chilled water tank firstly flows into the *evaporator 2* and pushes the residual chilled water inside the *evaporator 2* into the *evaporator 1*. Since temperature of the residual chilled water is higher than that of the *evaporator 1*, the *evaporator 1* is heated. At the same time, the *evaporator 2* is cooled by the chilled water. Since pressure drops in the right vacuum chamber, the *adsorber 2* continues to desorb water (refrigerant); while the *adsorber 1* keeps on adsorbing refrigerant due the raise of pressure in the left vacuum chamber. This process obtains similar effect as a conventional mass recovery process. Finally the chilled water flows back to the chilled water tank through V8. During this process, the *adsorber 2* is still heated by hot water while the *adsorber 1* is cooled by cooling water.

3) Heat recovery from adsorber 2

The valves V1, V4, V6 and V8 are switched when the second process is finished. Chilled water flows through the *evaporator 2* via V5 and back to the chilled water tank through V6. At the same time, hot water passes through the *adsorber 1* via V4, and temperature of the hot water drops due to the desorption of refrigerant in the *adsorber 1*. Then the hot water flows into the cooling tower via V2 and is cooled by spray water and airflow. Afterwards the hot water is heated by condensation of the water vapor in the left vacuum chamber while flowing through the *condenser 1*. Finally the hot water is further heated in the *adsorber 2* and flows back to the hot water tank via V3. Therefore temperature of the *adsorber 2* decreases. In conclusion, heat is recovered from the *adsorber 2* by the circulation of hot water.

4) Adsorber 1 operates in desorption process and adsorber 2 works in adsorption process

During this process, the *adsorber 1* is heated by hot water while the *adsorber 2* is cooled by cooling water coming from the *condenser 1*.

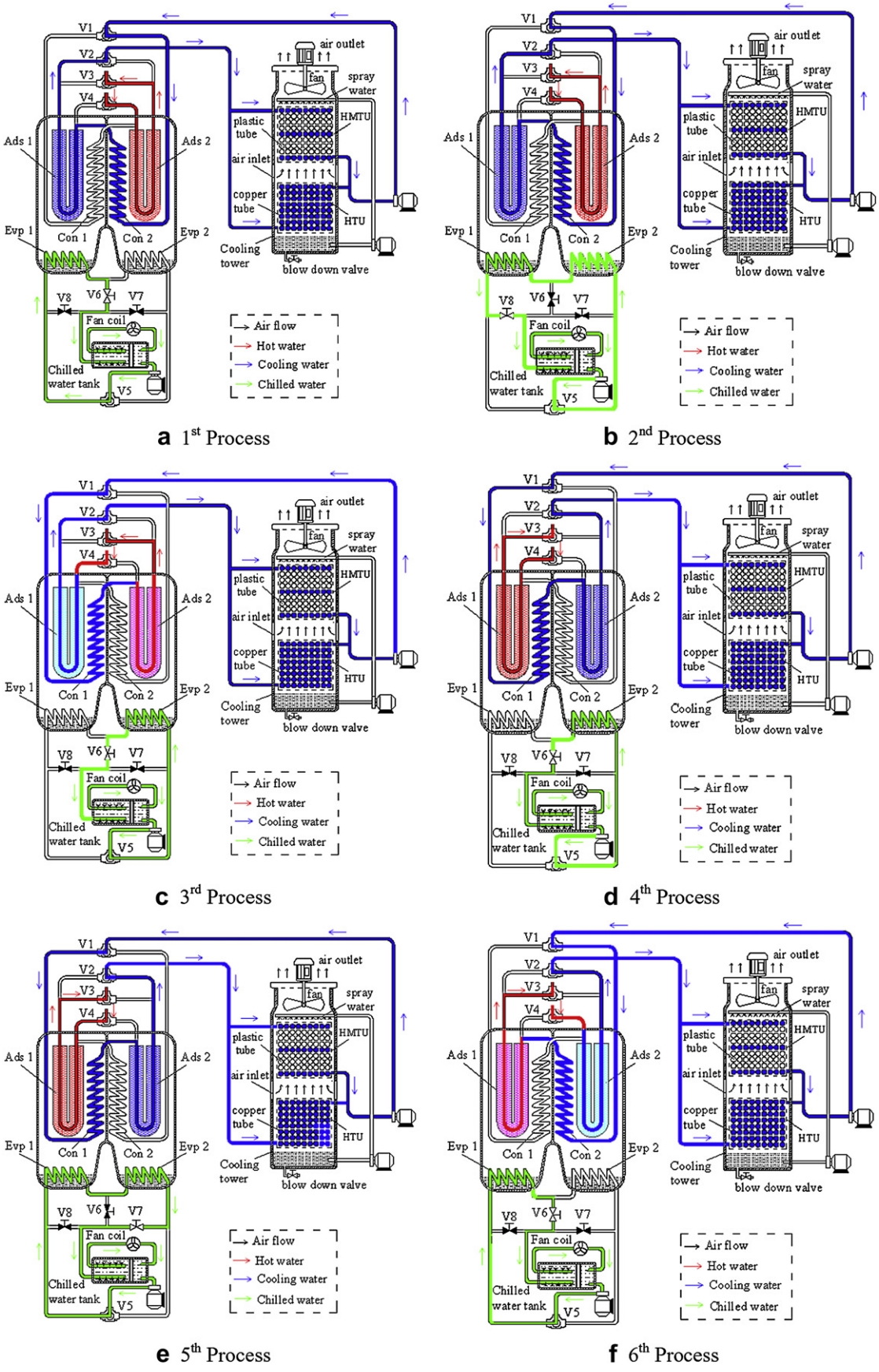

Fig. 2. Schematic drawing of the working processes of the studied adsorption chiller.

In the left vacuum chamber, water vapor desorbed is condensed in the *condenser 1* and the condensate flows into the *evaporator 1*. Simultaneously, water in the *evaporator 2* is adsorbed by the *adsorber 2* so that the chilled water passing through the *evaporator 2* is cooled. In this process, the *condenser 2* and the *evaporator 1* become idle.

5) Mass recovery-like process (Heat recovery from evaporator 1 to evaporator 2)

This process is similar to the second one. Chilled water flows through the *evaporator 1* and the *evaporator 2* in sequence, and finally runs back to the chilled water tank. During this step, the *evaporator 1* is cooled while the *evaporator 2* is heated. Thus the *adsorber 1* and the *adsorber 2* keep on desorbing and adsorbing refrigerant respectively in this process. As a result, the cycle mass of refrigerant is enlarged.

6) Heat recovery from adsorber 1

During this process, hot water flows firstly into the *adsorber 2* and is quickly cooled. Then the hot water is cooled by the spray water and airflow while going through the cooling tower. Afterwards the hot water flowing into the *condenser 2* is heated by the condensation of the water vapor desorbed by the *adsorber 2*. Finally the hot water is heated in the *adsorber 1* and flows back to the hot water tank.

When the 6th process is finished, the adsorption chiller goes to the 1st process and a new cycle begins.

4. Mathematical model

The main assumptions made on the adopted mathematical model are as follows:

1) The pressure of water vapor in the vacuum chamber is uniform.
2) The specific heat of the fluids is assumed to be constant. All the thermodynamic properties of water and water vapor were obtained from Wagner and Kruse [12]. Properties of the airflow are calculated from the property equations given by Feddaoui et al. [13].
3) Compared to the convection term, the diffusion term in the working fluid energy balance equations is much smaller so that it is neglected.
4) The spray water film with a constant film thickness covers all the wall of the tubes. And the interface temperature between the spray water film and the air is considered to be equal to the spray water film temperature.
5) The air and the spray water are uniformly distributed in the plane perpendicular to the flow, and the heat and mass transfer occurs only in the direction normal to the flow.
6) Mass of spray water taken away by the airflow per unit time is much smaller compared to the mass flow rate of the spray water. Therefore the mass flow rate of the spray water is assumed to be constant.
7) The heat exchange between the studied adsorption chiller and the surroundings is negligible.

4.1. Adsorption isotherm and adsorption rate

The adsorption equilibrium equation, which is a modified Freundlich equation [14], is adopted and shown in Eq. (1). Parameters of the equation for silica gel–water adsorption refrigeration working pair were obtained by Xia et al. [15].

$$X^* = A(T_a) \times \left[\frac{P(T_{cham})}{P(T_a)}\right]^{B(T_a)} \tag{1}$$

$$A(T_a) = -14.2904 + 0.1546T_a - 5.5498 \times 10^{-4}T_a^2 + 6.7512 \times 10^{-7}T_a^3$$

$$B(T_a) = 36.1487 - 0.3820T_a + 1.3016 \times 10^{-3}T_a^2 - 1.4150 \times 10^{-6}T_a^3$$

The adsorption rate can be expressed by the conventional linear driving force equation:

$$\frac{dX}{d\tau} = 15D_{so}\exp(-E_a/RT_a)/R_p^2 \cdot (X^* - X) \tag{2}$$

4.2. Adsorber

The adsorbers are fin-tube heat exchangers with the adsorbent filled in the fin space. During the calculation, mathematical model for the fins is canceled but the heat transfer coefficient between the adsorbent and the heat exchange tube is enlarged due to the integration of fins with the heat exchange tube. As is shown in Fig. 3, the adsorbers are simplified to three parts: adsorbent, the adsorber heat exchanger metal and the working fluid (hot water or cooling water).

Energy balance equation for the adsorbent is given by:

$$(M_aC_{p,a} + M_aXC_{p,wv})\frac{\partial T_a}{\partial \tau} = (hA)_{a,ad}(T_{ad} - T_a) + M_a\Delta H\frac{dX}{d\tau} \tag{3}$$

Energy balance equation for metal of the heat exchange tube in the adsorbers is:

$$M_{ad}C_{p,ad}\frac{\partial T_{ad}}{\partial \tau} = (hA)_{a,ad}(T_a - T_{ad}) + (hA)_{ad,f}(T_{f,ad} - T_{ad}) \tag{4}$$

Energy balance equation for the adsorber working fluid is:

$$M_{f,ad}C_{p,f}\frac{\partial T_{f,ad}}{\partial \tau} + G_{f,ad}C_{p,f}l_{ad}\frac{\partial T_{f,ad}}{\partial x} = (hA)_{ad,f}(T_{ad} - T_{f,ad}) \tag{5}$$

Initial conditions and boundary conditions:

$$T_{f,ad}|_{x=0} = T_{f,ad}|_{in} = \begin{cases} T_{hot}|_{in} & \text{desorption} \\ T_{f,c}|_{out} & \text{adsorption} \end{cases} \tag{6}$$

$$T_a = T_{ad} = T_{f,ad} = T_i \quad \tau = 0 \tag{7}$$

4.3. Condenser

The condensers used were the shell and tube heat exchangers and the shells of the vacuum chambers are also the shells of the

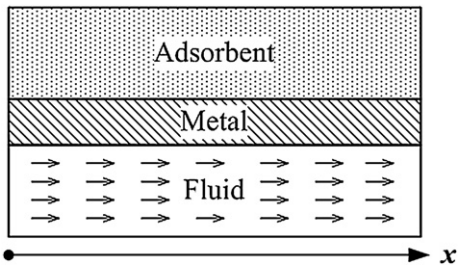

Fig. 3. Schematic diagram of heat exchange model for the adsorber.

condensers. The mathematical model for the condenser is divided into three parts: refrigerant, the condenser heat exchange tube metal and the working fluid.

Energy balance equation for condensation of the refrigerant is given as:

$$0 = (hA)_{c,cham}(T_{cham} - T_c) + M_a L\frac{dX}{d\tau} \quad T_{cham} \geq T_c \tag{8}$$

Energy balance equation for the condensers heat exchange tube metal is:

$$M_c C_{p,c}\frac{\partial T_c}{\partial \tau} = (hA)_{c,cham}(T_{cham} - T_c) + (hA)_{c,f}(T_{f,c} - T_c) \tag{9}$$

Energy balance equation for the condenser working fluid is:

$$M_{f,c}C_{p,f}\frac{\partial T_{f,c}}{\partial \tau} + G_{f,c}C_{p,f}l_c\frac{\partial T_{f,c}}{\partial x} = (hA)_{c,f}(T_c - T_{f,c}) \tag{10}$$

$$(hA)_{c,f} = \begin{cases} 4720.67 \times 2.22 & G_{f,c} \neq 0 \quad \text{Work} \\ 40 \times 2.22 & G_{f,c} = 0 \quad \text{Idle} \end{cases} \tag{11}$$

Initial conditions and boundary conditions are shown by the following equations:

$$T_{f,c}|_{x=0} = T_{f,c}|_{in} = T_{f,ct}|_{out} \tag{12}$$

$$T_c = T_{f,c} = T_i \quad \tau = 0 \tag{13}$$

4.4. Evaporator

The evaporators were the shell and tube heat exchangers and the shells of the vacuum chambers are also the shells of the evaporators. The mathematical model for evaporator is also divided into three parts: refrigerant, the evaporator heat exchange tube metal and the working fluid.

Energy balance equation for the evaporation of refrigerant can be given by:

$$0 = (hA)_{e,cham}(T_{cham} - T_e) + M_a L\frac{dX}{d\tau} \tag{14}$$

Energy balance equation for the evaporator heat exchanger tube metal is:

$$M_e C_{p,e}\frac{\partial T_e}{\partial \tau} = (hA)_{e,cham}(T_{cham} - T_e) + (hA)_{e,f}(T_{f,e} - T_e) \tag{15}$$

Energy balance equation for the evaporator working fluid is:

$$M_{f,e}C_{p,f}\frac{\partial T_{f,e}}{\partial \tau} + G_{f,e}C_{p,f}l_e\frac{\partial T_{f,e}}{\partial x} = (hA)_{e,f}(T_e - T_{f,e}) \tag{16}$$

$$(hA)_{e,f} = \begin{cases} 3000 \times 2.39 & G_{f,e} \neq 0 \quad \text{Work} \\ 35 \times 2.39 & G_{f,e} = 0 \quad \text{Idle} \end{cases} \tag{17}$$

Initial conditions and boundary conditions are shown as follows:

$$T_{f,e}|_{x=0} = T_{f,e}|_{in} = T_{chilled}|_{in} \tag{18}$$

$$T_e = T_{f,e} = T_i \quad \tau = 0 \tag{19}$$

4.5. Closed wet cooling tower

Heat and mass transfer in the HMTU and heat transfer in the HTU are shown in Fig. 4 (a) and Fig. 4 (b) respectively. The flowing direction of the three steams (cooling water, spray water and airflow) is also shown in Fig. 4. In the HMTU, cooling water releases heat to the metal of the copper tubes while the metal of the copper tubes is cooled by the spray water. At the same time, heat and mass transfer takes place between the spray water and the airflow. In the HTU, heat transfers from the cooling water to the spray water through the metal of the copper tubes.

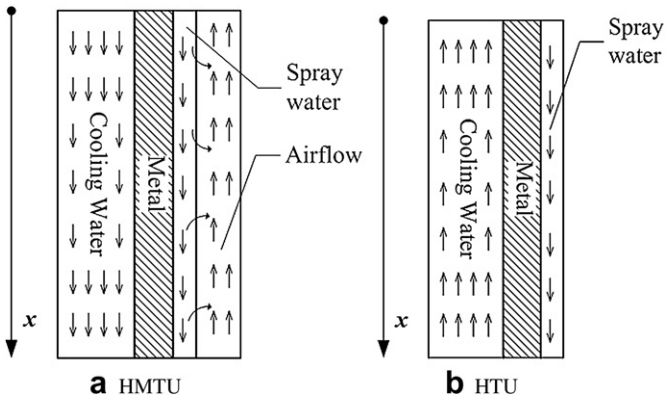

Fig. 4. Heat and mass transfer of the closed wet cooling tower (a) HMTU (b) HTU.

4.5.1. Energy balance equations and mass conversion equation in the HMTU

Energy balance equation for the cooling water is:

$$M_{f,hmtu}C_{p,f}\frac{\partial T_{f,hmtu}}{\partial \tau} + G_{f,hmtu}C_{p,f}l_{hmtu}\frac{\partial T_{f,hmtu}}{\partial x} = (hA)_{f,m}(T_{m,hmtu} - T_{f,hmtu}) \tag{20}$$

Energy balance equation for metal of copper tubes is given by:

$$M_{m,hmtu}C_{p,m}\frac{\partial T_{m,hmtu}}{\partial \tau} = (hA)_{f,m}(T_{f,hmtu} - T_{m,hmtu}) + (hA)_{sw,m}(T_{sw,hmtu} - T_{m,hmtu}) \tag{21}$$

There is a thin film of saturated air at the interface between the air and the spray water, which is in close contact with the spray water. Temperature of the thin film of saturated air is considered to be equal to that of the spray water. Since water vapor partial-pressure of the saturated air is larger than that of the airflow, water vapor transfers from the saturated air into the airflow. Simultaneously, there is a heat transfer process between the spray water and the airflow due to the temperature difference between the two steams. Thus energy balance equation for spray water can be expressed by the following equation:

$$M_{sw,hmtu}C_{p,sw}\frac{\partial T_{sw,hmtu}}{\partial \tau} + G_{sw,hmtu}C_{p,sw}l_{hmtu}\frac{\partial T_{sw,hmtu}}{\partial x} = (hA)_{sw,m}(T_{m,hmtu} - T_{sw,hmtu}) + (hA)_{sw,air}(T_{air} - T_{sw,hmtu}) - (\overline{hA})_{sw,air}(w_{sw} - w_{air})L \tag{22}$$

Energy balance equation for airflow is calculated as follows:

$$M_{air}C_{p,air}\frac{\partial T_{air}}{\partial \tau} - G_{air}C_{p,air}l_{hmtu}\frac{\partial T_{air}}{\partial x} = (hA)_{sw,air}(T_{sw,hmtu} - T_{air}) \tag{23}$$

Mass of water vapor changed in the airflow is given by:

$$M_{air}\frac{\partial w_{air}}{\partial \tau} - G_{air}l_{hmtu}\frac{\partial w_{air}}{\partial x} = (\overline{hA})_{sw,air}(w_{sw} - w_{air}) \tag{24}$$

Initial conditions and boundary conditions are shown as follows:

$$T_{f,hmtu}|_{x=0} = T_{f,hmtu}|_{in} \quad (25)$$

$$T_{sw,hmtu}|_{x=0} = T_{sw,hmtu}|_{in} \quad (26)$$

$$T_{air}|_{x=l_{hmtu}} = T_{air}|_{in} \quad (27)$$

$$w_{air}|_{x=l_{hmtu}} = w_{air}|_{in} \quad (28)$$

$$T_{f,hmtu} = T_{m,hmtu} = T_{sw,hmtu} = T_{air} = T_i \quad \tau = 0 \quad (29)$$

$$w_{air} = w_i \quad \tau = 0 \quad (30)$$

4.5.2. Energy conversion equations in the HTU

Energy balance equation for the cooling water is:

$$M_{f,htu}C_{p,f}\frac{\partial T_{f,htu}}{\partial \tau} + G_{f,htu}C_{p,f}l_{htu}\frac{\partial T_{f,htu}}{\partial x} = (hA)_{f,m}(T_{m,htu} - T_{f,htu}) \quad (31)$$

Energy balance equation for cooling tower metal is given by:

$$M_{m,htu}C_{p,m}\frac{\partial T_{m,htu}}{\partial \tau} = (hA)_{f,m}(T_{f,htu} - T_{m,htu}) + (hA)_{sw,m}(T_{sw,htu} - T_{m,htu}) \quad (32)$$

Energy balance equation for spray water can be expressed by the following equation:

$$M_{sw,htu}C_{p,sw}\frac{\partial T_{sw,htu}}{\partial \tau} + G_{sw,htu}C_{p,sw}l_{htu}\frac{\partial T_{sw,htu}}{\partial x} = (hA)_{sw,m}(T_{m,htu} - T_{sw,htu}) \quad (33)$$

Initial conditions and boundary conditions are shown as follows:

$$T_{f,htu}|_{x=l_{htu}} = T_{f,htu}|_{in} \quad (34)$$

$$T_{sw,htu}|_{x=0} = T_{sw,htu}|_{in} \quad (35)$$

$$T_{f,htu} = T_{m,htu} = T_{sw,htu} = T_i \quad \tau = 0 \quad (36)$$

4.6. Performance parameters equations

Cooling capacity:

$$Q_r = \frac{\int_0^{\tau_{cycle}} G_{f,e}c_{p,w}(T_{chilled,in} - T_{chilled,out})d\tau}{\tau_{cycle}} \quad (37)$$

Heating power:

$$Q_h = \frac{\int_0^{\tau_{cycle}} G_{f,ad}c_{p,w}(T_{hot,in} - T_{hot,out})d\tau}{\tau_{cycle}} \quad (38)$$

Coefficient of performance:

$$COP = \frac{Q_r}{Q_h} \quad (39)$$

Relative humidity of air can be given by [16]:

$$\varphi = 0.6207 \times \frac{P_{wv}}{1.01325 \times 10^5 - P_{wv}} \quad (40)$$

The partial differential equations were numerically solved using the finite difference method. The convection terms were calculated by an upwind difference formula and the unsteady terms were approximated by an implicit difference scheme. The computational domain was divided into 100 equal step discrete elements and the calculated time step was 1 s. For the major components of the chiller (adsorbers, evaporators and condensers), mass difference between water vapor adsorbed or desorbed by the adsorbent and the water vapor evaporated or condensed in the same chamber should be equal to zero. During the calculation, tolerance of the mass difference of water vapor was set to be 1×10^{-5} kg. Moreover, tolerance of the maximum temperature difference during the iterations was 1×10^{-3} K. Based on the initial conditions and the boundary conditions, temperature profiles of all the components of the chiller can be obtained. All the parameters used in the simulation are listed in Table 1.

5. Results and discussions

5.1. Validation data

Based on the structure and the operating processes of the chiller developed by Liu et al. [11], this mathematical model has been validated with the obtained experimental data. Fig. 5 shows the comparisons of the simulated results and experimental results under different chilled water inlet temperatures at the hot water inlet temperatures of 85 °C and the cooling water temperature of 28 °C. It can be observed that the predicted results agree well with the experimental measurement. Since the adopted mathematical model neglects heat transfer between the adsorption chiller and ambient, the calculated results are a little larger than the experimental data. The predicted cooling capacity and COP are 7.47 kW and 0.45 respectively while the experimental cooling capacity and COP are 7.13 kW and 0.42 respectively at the chilled water inlet temperature of 16.0 °C (shown in Fig. 5 (b)). The maximum relative

Table 1
Values for the parameters adopted in the simulation.

Parameters	Values	Units
D_{so}	2.54×10^{-4}	m s^{-2}
E_a	4.2×10^4	J mol^{-1}
$(hA)_{a,ad}$	90×59.33	W K^{-1}
$(hA)_{ad,f}$	2913.66×6.34	W K^{-1}
$(hA)_{c,cham}$	4200×2.53	W K^{-1}
$(hA)_{e,cham}$	3500×3.15	W K^{-1}
$(hA)_{f,m}$	3570.12×7.76	W K^{-1}
$(hA)_{sw,m}$	6732.14×8.37	W K^{-1}
$(hA)_{sw,air}$	54.49×34.08	W K^{-1}
$(\overline{hA})_{sw,air}$	0.054×34.08[a]	kg s^{-1}
M_a	65	kg
M_{ad}	169.77	kg
$M_{f,ad}$	16.04	kg
M_c	63.90	kg
$M_{f,c}$	6.02	kg
M_e	64.9	kg
$M_{f,e}$	8.8	kg
M_{air}	0.33	kg
$M_{f,hmtu}$, $M_{f,htu}$	17.11	kg
$M_{m,hmtu}$, $M_{m,htu}$	25.21	kg
$M_{sw,hmtu}$	5.60	kg
$M_{sw,htu}$	1.40	kg
R	8.3145	J mol^{-1} K^{-1}
R_p	3.75×10^{-4}	m

[a] Means that the mass transfer coefficient is calculated by assuming $Le = 1$.

error between the calculated cooling capacities and the corresponding experimental cooling capacities is about 5.3% while it is about 6.5% for the predicted COPs and the corresponding experimental COPs. As a result, this mathematical model is quite reliable in predicting performance of the silica gel–water adsorption chiller.

5.2. Temperature profiles of the working fluids and the relative humidity of the airflow

Fig. 6 (a) shows the outlet temperature profiles of the hot water, chilled water and the cooling water passing through the condenser, while the outlet temperature and relative humidity of the airflow can be observed in Fig. 6 (b). The inlet temperatures for hot water and chilled water are 85 and 15 °C respectively; together with the air inlet dry bulb temperature and wet bulb temperature of 30 and 28 °C respectively.

At the beginning of the desorption process, the desorbed refrigerant is condensed in the evaporator since the temperature of the evaporator is smaller than that of the condenser. Since the chilled water does not flow through the evaporator, the residual chilled water in the evaporator is heated. When the temperature of the evaporator is equal to that of the condenser, the desorbed refrigerant is condensed in the condenser and then the refrigerant condensate flows into the evaporator. Thus the residual chilled water is heated by the condensate. As a result, the fluid temperature of the evaporator is higher than that of the condenser during the desorption process (shown in Fig. 6 (a)). However, the temperature difference between the evaporator and condenser is decreased during the desorption process. The reason is that parts of

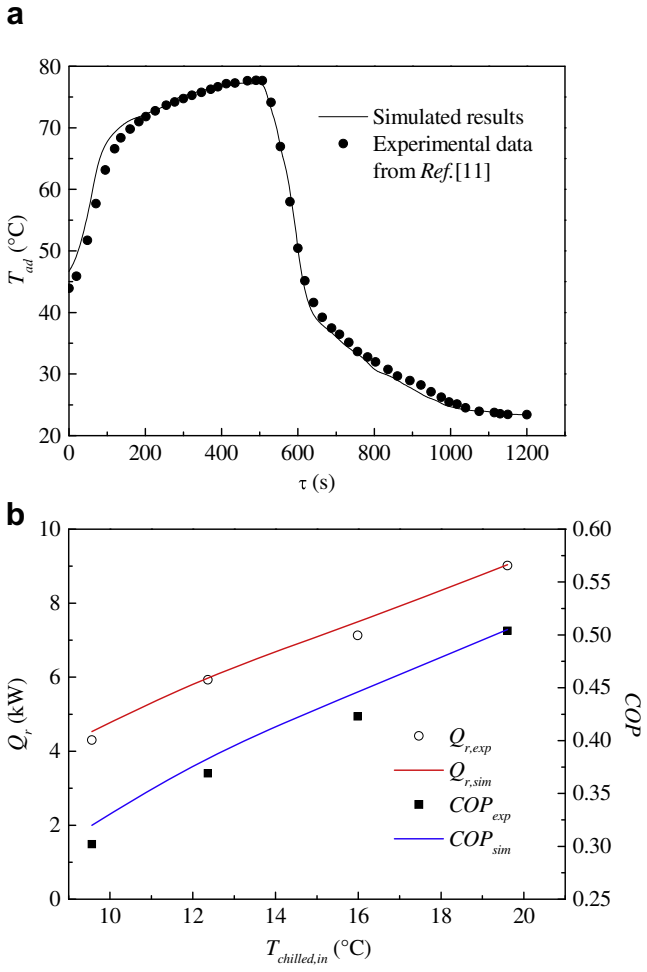

Fig. 5. Comparisons of the simulated result and the experimental data (a) Experimental and predicted temperature profiles of the adsorber studied in Ref. [11] (b) Cooling capacities and COPs under different chilled water inlet temperatures.

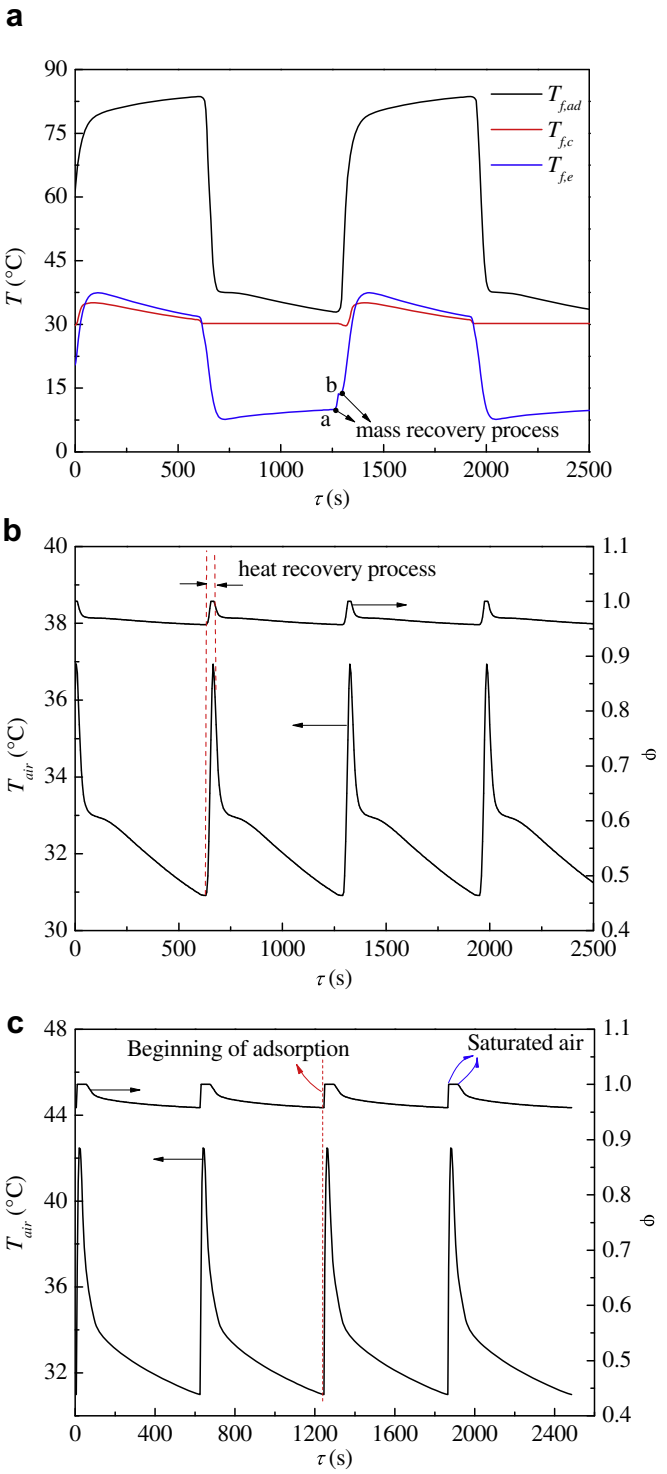

Fig. 6. Temperature profiles of the working fluids together with the outlet relative humidity of the airflow. (a) The outlet temperature of the working fluids passing through adsorber, condenser and evaporator (b) The outlet temperature profile and relative humidity of the airflow with heat and mass recovery (c) The outlet temperature profile and relative humidity of the airflow without heat recovery process.

refrigerant condensate in the evaporator evaporates and condenses in the condenser, then flows back to the evaporator again. During the adsorption process, the condenser in the adsorption chamber is idle. As a result, temperature of the residual cooling water in the condenser remains constant (in Fig. 6(a)). The chilled water passes through the evaporator in the adsorption chamber and is cooled.

Mass recovery-like process is carried out (shown in Fig. 6(a) form point 'a' to point 'b'). The chilled water with inlet temperature of 15 °C flows into the evaporator in the desorption chamber and is heated, then the heated chilled water passes through the evaporator in the adsorption chamber and is cooled, finally returns back to the chilled water tank. As is shown in Fig. 6(a), the outlet temperature of chilled water passing through the evaporator of the adsorption chamber is smaller than 15 °C. It means that the output of cooling capacity is obtained during the mass recovery-like process, which is quite different form conventional mass recovery processes [10,17].

As is shown in Fig. 6(b), the relative humidity of outlet air is about 96% (0.96) while it is increased to 100% during the heat recovery process. As mentioned in section 3, during the heat recovery process hot water flows into the adsorber, which will desorb refrigerant next step; temperature of the hot water is greatly decreased after flowing through the adsorber, and then it passes through the cooling tower. In the cooling tower, hot water with a low temperature releases heat to spray water through the copper tubes. Thus the spray water is heated. When air flows through the cooling tower, it is heated by the spray water due to the temperature difference between the two steams. Since temperature of the spray water is increased, water vapor partial-pressure in the saturated air at the interface between the air and the spray water rises. Due to the large water vapor pressure difference between the saturated air at the interface and the airflow, water vapor moves into the airflow. As a result, the outlet airflow becomes saturated.

The temperature profile and the relative humidity of the outlet airflow without heat recovery process are also shown in Fig. 6(c). After the mass recovery process, temperature of the residual hot water in the desorber is almost equal to the inlet hot water temperature. When the adsorption process begins, the residual hot water in the desorber, which will be in adsorption process, rushes into the cooling tower. Therefore, the spray water is heated by the residual hot water. Then spray water releases heat to the airflow; furthermore, some spray water evaporates into the airflow due to the water vapor partial-pressure difference between the saturated air at the interface and the airflow. As a result, temperature of the airflow is sharply increased at the beginning of adsorption. Since the spray water temperature is high, large amount of spray water moves into the airflow. Thus the outlet airflow has been saturated for a period of time. As shown in Fig. 6(b) and Fig. 6(c), the outlet temperature of the airflow without heat recovery process is larger than that with heat recovery process at the beginning of adsorption process.

5.3. Determination of the optimum cycle time

Fig. 7 presents the effects of adsorption/desorption time on COP and cooling capacity when the mass recovery-like time and heat recovery time are 20 and 40 s respectively. It is clearly shown that COP increases with the adsorption/desorption time due to the decrease of the heating power of the adsorber. The cooling capacity increases steeply when the adsorption/desorption time is smaller than 600 s, and it decreases with a smaller slope for the adsorption/desorption time over 600 s. A lower cooling capacity is obtained under a shorter adsorption/desorption time due to the insufficient heating to the desorber and cooling to the adsorber. A maximum cooling capacity is achieved when the adsorption/desorption time is about 600 s. The cycle mass of refrigerant increases slightly,

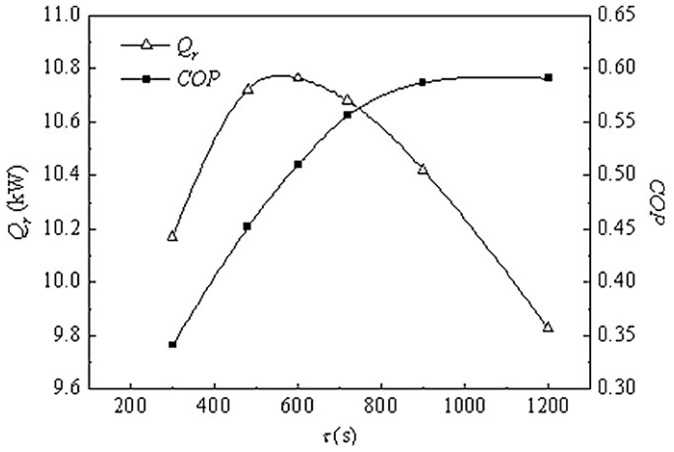

Fig. 7. Cooling capacities and COPs of the studied chiller under different adsorption/desorption time.

which results in a decrease of cooling capacity, when the adsorption/desorption time is over 600 s. The cooling capacity and COP are 10.76 kW and 0.51 respectively when the adsorption/desorption time is 600 s. The cooling capacity is decreased by 8.7% and COP is increased by 18.2% when the adsorption/desorption time changes from 600 to 1200 s.

5.4. Comparisons of heat and mass recovery cycle and basic cycle

Fig. 8 shows the chamber temperature versus the adsorbent temperature for the heat and mass recovery cycle and basic cycle. Curves 'ab' and 'de' denote the mass recovery-like process. Curves 'bc' and 'ef' mean the heat recovery process. Curves 'cd' and 'fa' are the desorption and adsorption processes, respectively. During the mass recovery-like process, chilled water flows through the evaporators in desorption chamber and adsorption chamber in sequence. Thus the desorber in the desorption chamber continues to desorb refrigerant due to the pressure drop of desorption chamber, while the adsorber in the adsorption chamber keeps on absorbing refrigerant from the evaporator due to the increase of chamber temperature. As is shown in Fig. 8, water uptake of the adsorber is increased from 0.139 to 0.150 while water uptake of the desorber is changed from 0.076 to 0.065. Compared with the basic

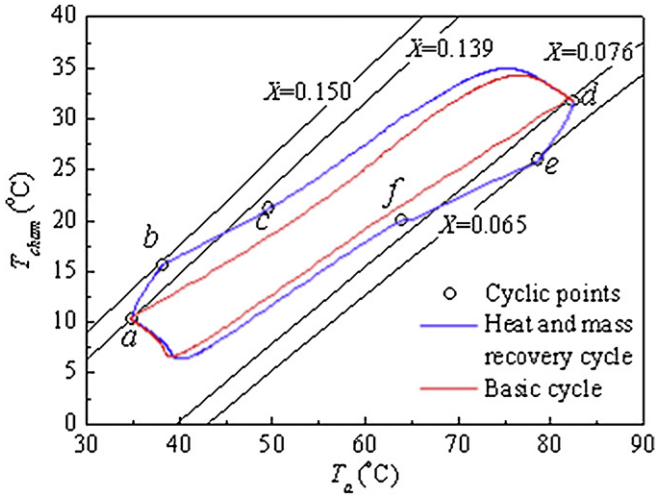

Fig. 8. Comparison of heat and mass recovery cycle and basic cycle.

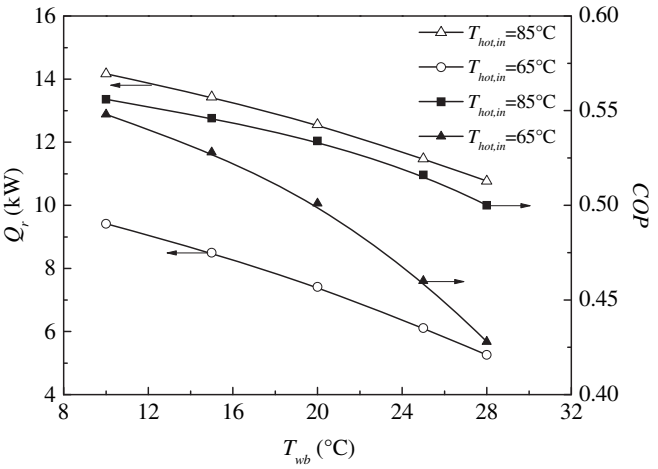

Fig. 9. Cooling capacities and COPs under different inlet air wet bulb temperatures with the inlet dry bulb temperature of 30 °C.

cycle, the cycle mass of the heat and mass recovery cycle is increased by 34.9%. After the mass recovery-like process, a heat recovery process is carried out. The residual hot water in the desorber, which will be in adsorption process next step, is recycled to enhance the COP of the chiller.

5.5. Effect of the inlet air conditions

For the studied adsorption chiller, cooling water flowing through the chiller is cooled by the spray water in the closed wet cooling tower. And temperature of the spray water is dominated by the heat and mass transfer between the spray water and airflow. Spray water is heated by the cooling water coming from the adsorption chiller. When air flows through the tube bundles, temperature of the spray water drops due to the evaporation of spray water into the airflow. With the decrease of air inlet wet bulb temperature, relative humidity of the inlet airflow is lessened, which results in a larger amount of spray water vapor transferred into the airflow. As a result, a smaller cooling water temperature can be obtained with the decrease of air inlet wet bulb temperature. Influence of wet bulb temperature on the chiller is shown in Fig. 9. When the hot water inlet temperature is 85 °C, the cooling capacity and COP are increased by 31.6% and 11.2% respectively with the decrease of wet bulb temperature from 28 to 10 °C. For the hot water inlet temperature of 65 °C, the cooling capacity and COP are increased by 78.9% and 28.0% respectively when the wet bulb temperature is decreased from 28 to 10 °C. It can be observed that the air inlet wet bulb temperature has a larger influence on the performance of the studied adsorption chiller at a lower heat source temperature. The reason is that both the desorption process and adsorption process are insufficient if a small heat source temperature and a high air inlet wet bulb temperature are adopted, which results in a small cycle mass.

6. Conclusions

A silica gel–water adsorption chiller integrated with a closed wet cooling tower was developed and numerically studied. A transient one-dimensional model was proposed and validated using experimental data. The predicted results agreed well with the experimental measurement. Based on this reliable mathematical model, the following conclusions were achieved:

1) Under typical working conditions, which are the hot water and chilled water inlet temperatures of 85 and 15 °C respectively, together with the air inlet dry bulb temperature and wet bulb temperature of 30 and 28 °C respectively, the cooling capacity and COP of the chiller are 10.76 kW and 0.51, respectively.
2) From the outlet temperature profiles of chilled water, output of cooling capacity is obtained during the mass recovery-like process, which is quite different from a conventional mass recovery process. Compared with basic cycle, the cycle mass of heat and mass recovery cycle is increased by 34.9%.
3) The air inlet wet bulb temperature has a larger influence on the performance of the studied chiller if a lower heat source temperature is adopted. When the wet bulb temperature is changed from 28 to 10 °C, the cooling capacities at the hot water inlet temperatures of 85 and 65 °C are increased by 31.6% and 78.9% respectively, while the COPs of the chiller at the hot water inlet temperatures of 85 and 65 °C are enlarged by 11.2% and 28.0%, respectively.

Acknowledgements

This work was supported by the national 863 Program (HI-TECH RESEARCH AND DEVELOPMENT PROGRAM OF CHINA) under the contract No. 2006AA05Z413, and also the Research Fund for the Doctoral Program of Higher Education under the contract No. 20070248023.

References

[1] X.L. Wang, H.T. Chua, Two bed silica gel–water adsorption chillers: an effectual lumped parameter model. Int. J. Refrig. 30 (2007) 1417–1426.
[2] B.B. Saha, E.C. Boelman, T. Kashiwagi, Computer simulation of a silica gel–water adsorption refrigeration cycle – the influence of operating conditions on cooling output and COP. ASHRAE Trans. Res. 101 (1995) 348–357.
[3] H.T. Chua, K.C. Ng, W. Wang, C. Yap, X.L. Wang, Transient modeling of a two-bed silica gel–water adsorption chiller. Int. J. Heat Mass Trans. 47 (2004) 659–669.
[4] B.B. Saha, A. Chakraborty, S. Koyama, Y.I. Aristov, A new generation cooling device employing $CaCl_2$-in-silca gel–water system. Int. J. Heat Mass Trans. 52 (2009) 516–524.
[5] J. Di, J.Y. Wu, Z.Z. Xia, R.Z. Wang, Theoretical and experimental study on characteristics of a novel silica gel–water chiller under the conditions of variable heat source temperature. Int. J. Refrig. 30 (2007) 515–526.
[6] R.Z. Wang, T.S. Ge, C.J. Chen, Q. Ma, Z.Q. Xiong, Solar sorption cooling systems for residential applications: options and guidelines. Int. J. Refrig. 32 (2009) 638–660.
[7] P. Stabat, D. Marchio, Simplified model for indirect-contact evaporative cooling-tower behavior. Appl. Energ. 78 (2004) 433–451.
[8] A. Hasan, K. Sirén, Theoretical and computational analysis of closed wet cooling towers and its applications in cooling of buildings. Energ. Buildings. 34 (2002) 477–486.
[9] J.M. Wu, X. Huang, H. Zhang, Theoretical analysis on heat and mass transfer in a direct evaporative cooler. Appl. Therm. Eng. 29 (2009) 980–984.
[10] D.C. Wang, J.Y. Wu, Z.Z. Xia, H. Zhai, R.Z. Wang, W.D. Dou, Study of a novel silica gel–water adsorption chiller. Part II. Experimental study. Int. J. Refrig. 28 (2005) 1084–1091.
[11] Y.L. Liu, R.Z. Wang, Z.Z. Xia, Experimental study on a continuous adsorption water chiller with novel design. Int. J. Refrig. 28 (2005) 218–230.
[12] W. Wagner, A. Kruse, Properties of Water and Steam. Science Press, Beijing, 2003, (Translated by Xiang H.W.).
[13] M. Feddaoui, A. Mir, E. Belahmidi, Cocurrent turbulent mixed convection heat and mass transfer in falling film of water inside a vertical heated tube. Int. J. Heat Mass Trans. 46 (2003) 3497–3509.
[14] B.B. Saha, E.C. Boelman, T. Kashiwagi, Computational analysis of an advanced adsorption-refrigeration cycle. Energy 20 (1995) 983–994.
[15] Z.Z. Xia, C.J. Chen, J.K. Kiplagat, R.Z. Wang, J.Q. Hu, Adsorption equilibrium of water on silica gel. J. Chem. Eng. Data 53 (2008) 2462–2465.
[16] H.B. Bacha, M. Bouzguenda, M.S. Abid, A.Y. Maalej, Modeling and simulation of a water desalination station with solar multiple condensation evaporation cycle technique. Renew. Energ. 18 (1999) 349–365.
[17] R.Z. Wang, Performance improvement of adsorption cooling by heat and mass recovery operation. Int. J. Refrig. 24 (2001) 602–611.